# Optimization of Material and Operational Costs in Electromagnet Design

**Areg Grigoryan**
Automation and Electromagnetic Systems Research Laboratory, National Polytechnic University of Armenia, Armenia
grigoryan@polytechnic.am

**Armine Avetisyan**
Automation and Electromagnetic Systems Research Laboratory, National Polytechnic University of Armenia, Armenia
arm.avetisyan@seua.am (corresponding author)

**Lida Harutyunyan**
National Polytechnic University of Armenia, Armenia
lidaharutyunyan3@gmail.com

*Received: 4 August 2025 | Revised: 19 September 2025 | Accepted: 27 September 2025*

 *DOI: https://doi.org/10.48084/etasr.13826*

## ABSTRACT

**This study addresses the problem of optimizing the design of an electromagnet with a straight armature by considering both material and operational costs. A hybrid optimization framework was developed, combining traditional heuristic optimization techniques with machine learning-based models. Neural networks were trained on a dedicated database to predict the objective functions, namely material cost and power consumption, as functions of the design variables and the temperature of the control coil winding. The performance metrics for the predictive models demonstrate high accuracy ($R^2 > 0.9$). Both single-objective and multi-objective formulations were analyzed, with multi-objective optimization implemented through a weighted scalar function. The proposed method enables an efficient search for optimal solutions while reducing computational effort. The results confirm the potential of integrating data-driven models with optimization strategies in the design of cost-effective and energy-efficient electromagnetic systems. The proposed framework provides designers with a structured, data-driven approach for balancing manufacturing costs and operational efficiency.**

***Keywords-electromagnet with a straight armature; material cost; operational cost; hybrid optimization; heuristic optimization algorithms; machine learning***

## I. INTRODUCTION

Electromagnets are critical components in a wide range of electromechanical systems, including actuators, brakes, motors, magnetic separators, and lifting devices. Their performance directly impacts the functionality, reliability, and energy efficiency of these systems. Electromagnet design primarily focuses on achieving functional objectives such as magnetic field intensity, response speed, or torque output. However, the increasing demands for cost-effectiveness, sustainability, and power efficiency have positioned electromagnet design as a multi-objective optimization problem, where technical performance must be balanced with economic constraints.

Material and operational costs are among the key optimization criteria. Material cost is determined by the type and volume of components used, particularly copper for the control coil and soft or hard magnetic materials. Operational cost, on the other hand, relates to resistive losses, electromagnetic inefficiencies, and long-term energy consumption. Suboptimal choices in geometry or coil design can lead to excessive manufacturing costs and reduced energy efficiency.

Various optimization techniques have been applied to address these challenges. Metaheuristic techniques, such as Genetic Algorithms [1], Kriging-assisted surrogate models [2], and Gaussian process-based adaptive sampling [3], have been used to reduce losses and magnet cost while maintaining performance. In [4], a dual-objective optimization method was proposed for DC coils considering both power loss and manufacturing cost. Authors in [5] discussed how machine learning methods, including neural networks, support vector machines, and deep learning, can predict electromagnetic characteristics and guide efficient design.

Structural and system-level enhancements have been explored. Authors in [6] presented an axial-field, coreless tidal energy generator, optimized for low-velocity environments, while authors in [7] highlighted the importance of multi-objective optimization and control techniques for Axial-Flux Permanent Magnet (AFPM) motors. In [8], a multi-physics framework combining electromagnetic, thermal, and mechanical simulations was used to optimize toroidal superconducting magnets. The design of externally excited synchronous motors with improved rotor topology was presented in [9], aiming to enhance torque ripple and reduce electromagnetic losses.

In [10], an analytical and FEM-assisted optimization approach was used to design High-Temperature Superconducting (HTS) solenoids with maximum energy density. A mathematical formulation was introduced for determining the critical current of solenoid coils and validated through simulations conducted in MATLAB and COMSOL environments. In addition, the importance of combining simulation and analytical tools for optimizing advanced magnetic systems, such as Magnetic Resonance Imaging (MRI) and Superconducting Magnetic Energy Storage (SMES), was highlighted.

The optimization of high-end magnetic systems, such as superconducting coils used in MRI or SMES, has also been extensively studied. In [11], a linear–nonlinear optimization procedure was applied to minimize superconductor volume while preserving field uniformity. In [12], multi-objective evolutionary algorithms were implemented to reduce mechanical stress and improve energy density in HTS-SMES systems. A detailed review of optimization strategies for superconducting solenoidal magnets was provided in [13], which categorized the literature based on the objective type, technique, and application. It was also emphasized that many modern techniques are still underutilized.

Additive manufacturing and topology optimization have expanded the range of feasible solutions in electromagnet design. For example, authors in [14] evaluated the maturity of printed copper and magnetic materials, while authors in [15] reviewed how solid mechanics–based topology optimization methods are adapted for electromagnetic applications. Furthermore, the dual-coil model in [16] introduced energy-aware excitation strategies that enhance reliability and reduce operational cost.

In adjacent fields, heat dissipation and energy management challenges have also inspired novel optimization frameworks. In [17], inverse heat transfer problems were addressed using entropy-generation-minimizing strategies and metaheuristic optimization algorithms. Serial and parallel estimation approaches were proposed and validated through sensitivity analysis and statistical testing. The serial strategy proved to be more stable and reliable, demonstrating how thermal optimization strategies can be leveraged in electromagnetic applications.

In the context of intelligent power systems, authors in [18] analyzed hybrid SMES-hydrogen energy storage in smart grids, balancing economic constraints with grid stability. These examples underscore the growing importance of cost-aware and multi-domain optimization in the design of electromagnetic and energy conversion devices.

The costs incurred during both the production and operation phases of electromagnets can be reduced if the device structure is appropriately optimized during its design phase. In this study, single-objective optimization problems are formulated and solved to determine the minimum cost of the materials (steel and winding wire) used in the construction of an electromagnet with a straight armature and the minimum electric power of the control coil during operation (which corresponds to the minimum energy consumption or maximum energy efficiency). In addition, a bi-objective optimization problem is formulated and addressed.

## II. MATERIALS AND METHODS

The electromagnet under investigation is illustrated in Figure 1 [19]. A magnetic force $P_E$, generated by the current $I$ in the control coil, acts on the armature. When this force exceeds the opposing mechanical force $P_M$ acting on the armature, the latter moves toward the pole pieces of the core, thereby moving a mechanical load (the case in which $P_M$ remains constant regardless of the air gap $g$ is considered). The base, core, and armature are composed of soft magnetic steel material, while the control coil winding, consisting of $w$ turns, is made of copper wire.

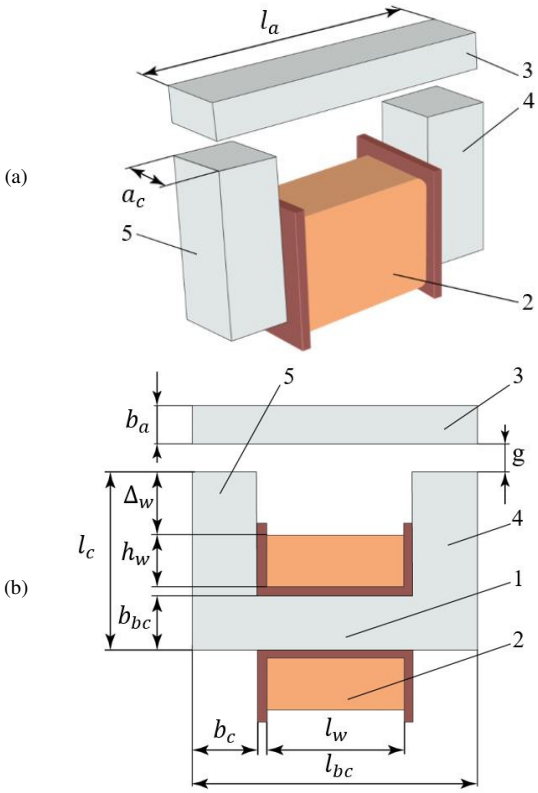


Fig. 1. Electromagnet: (a) and projected view of the electromagnet; (b), 1- base core, 2 - control coil, 3 - armature, 4, 5 – cores, $l_a$, $l_c$, $l_{bc}$, $b_a$, $b_c$, $b_{bc}$, $a_c$, $l_w$, $h_w$, $\Delta_w$ - structural dimensions.

In [19], the equivalent magnetic circuit of the electromagnet, its mathematical model, as well as the solution methods for the direct magnetic problem (where the magnetic flux $\Phi$ in the air gap is known and the magnetomotive force $F = Iw$ is determined) and the inverse problem (where $F$ is known and $\Phi$ is determined), are presented. The study described the automated system for the electromagnet design, where the input parameters include the mechanical force $P_M$, armature displacement $g_0$, and maximum ambient temperature $\theta_{max}$. The output parameters include all structural dimensions of the electromagnet, the types of materials used, magnetic fluxes, magnetic inductions, magnetic field intensities, electromagnetic force $P_E$ at various values of $g$, the magnetomotive force $F$, number of coil winding turns $w$, current $I$, power consumption $Q = IR^2$ (where $R$ is the coil resistance), temperature of the control coil, and material prices for copper wire and steel.

In [19], the following values were considered: $P_M = 15000\ N$, $g_0 = 0.01\ m$, $\theta_{max} = 40°C$, with *Steel C10* selected as the core material and *PSDKT* used as the control winding wire. The following two single-objective optimization problems for the electromagnet were formulated and solved:

1. Minimization of material cost (steel and winding wire):

$$V(K_c, K_{cc}, K_a,\ K_{bc}, K_\Delta, K_w, B_{g_0}) \Rightarrow \min \quad (1)$$

2. Minimization of power consumed by the control coil:

$$P\ (K_c, K_{cc}, K_a, K_{bc}, K_\Delta, K_w, B_{g_0}) \Rightarrow \min \quad (2)$$

where the structural coefficients are defined as: $K_c = \frac{b_c}{a_c}$, $K_{cc} = \frac{l_c}{a_c}$, $K_a = \frac{b_a}{b_c}$, $K_{bc} = \frac{b_{bc}}{b_c}$, $K_\Delta = \frac{\Delta_w}{l_c}$, $K_w = \frac{l_w}{h_w}$, and $B_{g_0}$ is the magnetic induction in the air gap when $g = g_0$.

The following constraints have been applied for the optimization problems:

$$\begin{cases} 1.0 \le K_c \le 1.1, \\ 1.5 \le K_{cc} \le 2.0, \\ 0.6 \le K_a \le 0.8, \\ 1.0 \le K_{bc} \le 1.1, \\ 0.02 \le K_\Delta \le 0.05, \\ 1.2 \le K_w \le 2.0, \\ 0.9 \le B_{g_0} \le 1.2(T), \\ \theta_c \le 160°\text{C}: \end{cases} \quad (3)$$

where $\theta c$ is the temperature of the control coil winding.

The optimization problems were solved using both a genetic algorithm and a hybrid approach, where the genetic algorithm was applied to a database trained with machine learning algorithms. This database comprises data from 1,000,000 designs generated by an automated design system. A similar approach was also adopted for the optimal design of a brake using magnetorheological fluid [20].

The formulated optimization problems belong to the class of nonlinear programming problems, where the analytical form of the objective function is unknown; hence it is not possible to compute the gradient vector components. For such problems, heuristic search methods are considered appropriate. These methods have been previously applied to optimize the force acting on the front of the particle bridge and the velocity of its movement in electromagnetic brakes with magnetorheological (MR) fluid, obtaining satisfactory results [21]. Moreover, for the optimal design of MR electromagnets, a hybrid approach combining heuristic and machine learning methods, has been applied. In that case, it was found that, compared to heuristic methods such as coordinate descent and hyperspherical methods, the hybrid optimization approach led to a nearly 30-times faster computation under identical hardware configurations. Therefore, this study also deploys hybrid methods to find the minimum values of $V$ and $P$.

## III. OPTIMIZATION RESULTS AND DISCUSSION

The single-objective optimization problems (1) and (2), subject to constraints (3), were solved using a hybrid approach that combines heuristic algorithms with machine learning models. First, the dataset was used to train various machine learning algorithms. The best performance for each target prediction task was achieved with the following neural network architectures:

- For predicting material cost ($V$): a three-layer neural network with layer sizes of 30, 20, and 10 neurons was employed, using the ReLU activation function. The model achieved the following performance metrics: RMSE = 3.579963, MSE = 12.816136, $R^2$ = 0.994435, and MAE = 2.426796.
- For predicting the power consumed by the control coil ($P$): a three-layer neural network with layer sizes of 200, 150, and 70 neurons was deployed, also using the ReLU activation function. The resulting performance metrics were: RMSE = 33.979473, MSE = 1.154604, $R^2$ = 0.9389982, and MAE = 13.806225.
- For predicting the temperature of the control coil winding ($\theta_c$): a three-layer neural network with layer sizes 30, 20, and 10 was utilized, using the ReLU activation function. The resulting performance metrics were: RMSE = 2.7826, MSE = 7.7427, $R^2$ = 0.90812, and MAE = 1.3145.

The choice of each neural network topology was guided by the complexity of the target variable. For $V$, the input–output mapping was relatively smooth and low-dimensional; thus, a compact three-layer architecture (30–20–10 neurons) provided sufficient accuracy. In contrast, predicting $P$ depended on the overall electromagnet design, coil geometry, and resistive losses, requiring a deeper architecture (200–150–70 neurons) to capture higher-order nonlinearities. Finally, predicting $\theta_c$ had a similar complexity to the material cost, where a smaller topology balanced accuracy with computational efficiency. This adaptive selection ensured high predictive performance while avoiding over-parameterization.

To solve optimization problems (1) and (2), a hybrid optimization strategy was implemented, combining heuristic techniques with machine learning prediction models. The search for the optimal solution was performed using two heuristic algorithms: coordinate descent and the hyperspherical methods. At each iteration, the values of the objective functions and the temperature $\theta_c$ were predicted using the pre-trained

machine learning models. All computations were implemented in the MATLAB environment, and extensive testing was conducted.

As a result of solving problem (1), the optimal value $V^*$, the corresponding optimal values of the structural coefficients, and the magnetic induction for the coordinate descent and hyperspherical methods are:

- Coordinate descent method:

$V^*$ = 178.63,with $K_c$ = 1.1, $K_{cc}$=1.6650 $K_a$ = 0.7036, $K_{bc}$ = 1.1, $K_\Delta$ = 0.050, $K_w$ = 1.51561, $B_{g0}$ =1.13

- Hyperspherical method:

$V^*$ = 177.51, with $K_c$ = 1.0983, $K_{cc}$ = 1.6458, $K_a$ = 0.7262, $K_{bc}$ = 1.099, $K_\Delta$ = 0.0497, $K_w$ = 1.6217, $B_{g0}$ = 1.126

Figure 2 shows the objective function surface as a function of two of the seven variables, $B_{g_{0_c}}$ and $K_c$, whereas the other five variables ($K_{cc}, K_a, K_{bc}, K_\Delta, K_w$) were kept constant. The red curve depicts the optimization path using the coordinate descent method within the hybrid framework, while the yellow curve shows the path using the hyperspherical method. The optimal solution for problem (1) was reached after 99 iterations using the coordinate descent method, and 90 iterations using the hyperspherical method. Figure 3 presents the objective function surface as a function of $K_\Delta$ and $K_{cc}$ along with the optimization paths (red and yellow lines) corresponding to the two methods.

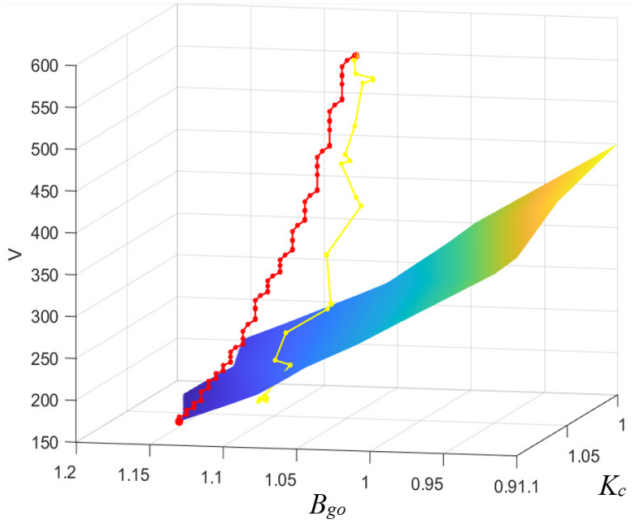


Fig. 2. Surface of the objective function $V(B_{go}, K_c)$ and the optimization paths.

Regarding problem (2), the optimal value $P^*$ was determined through a series of optimization experiments using two methods:

- Coordinate descent method:

$P^*$ = 1018.56, with $K_c$ = 1.09630514, $K_{cc}$ = 1.800000, $K_a$ = 0.75426469, $K_{bc}$ = 1.1, $K_\Delta$ = 0.05, $K_w$ = 1.57423640, $B_{g0}$ = 1.00689573

- Hyperspherical method:

$P^*$ = 1031.93, with $K_c$ = 1.04856337, $K_{cc}$ = 1.71542663, $K_a$ = 0.68956006, $K_{bc}$ = 1.07604435, $K_\Delta$ = 0.03818641, $K_w$ = 1.5795777, $B_{g0}$ = 1.02246543

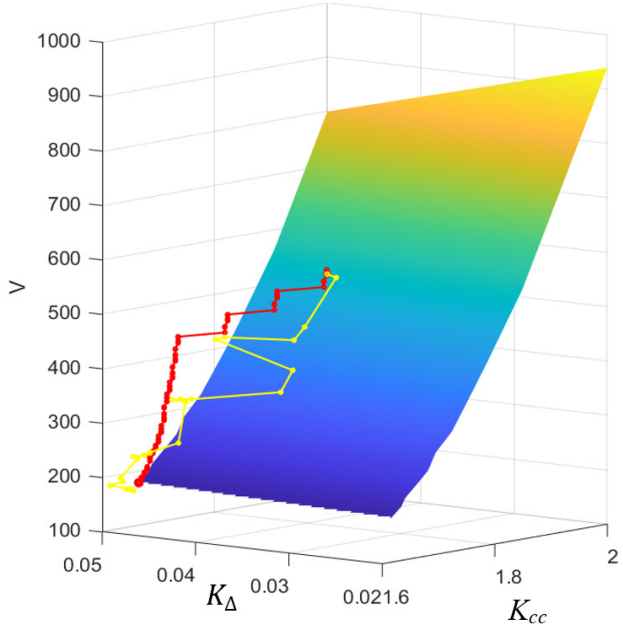


Fig. 3. Surface of the objective function $V(K_\Delta, K_{cc})$ and the optimization paths.

Figure 4 illustrates the optimization path using the coordinate descent method on the objective function surface defined by $K_c$ and $K_{cc}$, while the remaining five variables are held constant. Figure 5 shows the surface of the objective function $P_E(B_{go}, K_w)$, along with the optimization paths starting from the same initial point for both the coordinate descent (red line) and hyperspherical (yellow line) methods.

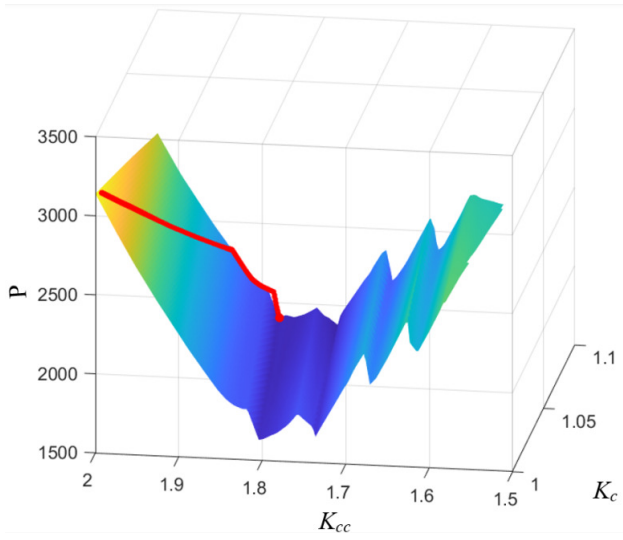


Fig. 4. Surface of the objective function $P(K_c, K_{cc})$ and the optimization paths.

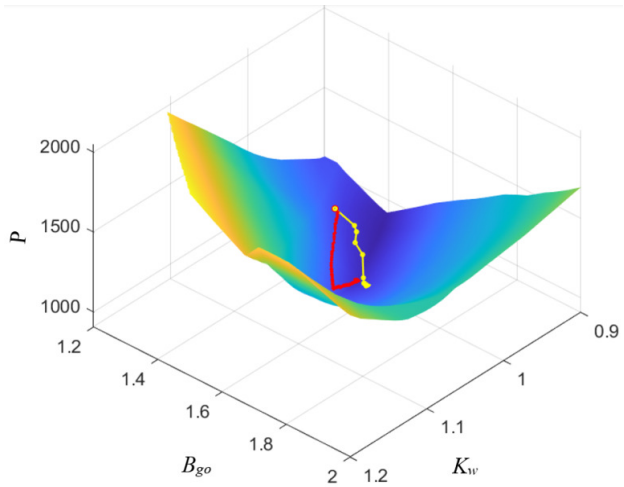


Fig. 5. Surface of the objective function $P(B_{go}, K_w)$ and the optimization paths.

In practical engineering design, it is often desirable to consider multiple objectives simultaneously. In this study, a bi-objective optimization problem is formulated by combining the two single-objective functions using the weighted sum method [22]. Since the two objectives, $V$ and $P$, have different physical units, they are first normalized before being aggregated into a composite scalar objective function:

Let,

$$V(X) = V(K_c, K_{cc}, K_a, K_{bc}, K_\Delta, K_w, B_{g_0}),$$

$$P(X) = P(K_c, K_{cc}, K_a, K_{bc}, K_\Delta, K_w, B_{g_0}),$$

$$f(X) = f(K_c, K_{cc}, K_a, K_{bc}, K_\Delta, K_w, B_{g_0})$$

The normalized functions are defined as:

$$V^{norm}(X) = \frac{V(X) - V^{min}}{V^{max} - V^{min}},$$

$$P^{norm}(X) = \frac{P(X) - P^{min}}{P^{max} - P^{min}},$$

where $V^{min}$, $V^{max}$, $P^{min}$, and $P^{max}$ are the minimum and maximum observed values of the respective functions from the dataset. The composite (scalar) objective function is then expressed as:

$$f(X) = \alpha V^{norm}(X) + (1 - \alpha) P^{norm}(X) ==> \min. \quad (4)$$

where $\alpha \in [0, 1]$ is the weight coefficient that reflects the relative importance of minimizing material cost versus power consumption. When $\alpha > 0.5$, material cost minimization is prioritized; when $\alpha < 0.5$, operational cost becomes more significant; and when $\alpha = 0.5$, both objectives are equally weighted. In the objective function (4), the normalization bounds were set as: $V_{min} = 177$, $V_{max} = 587$, $P_{max} = 2533$, $P_{min} = 1018$.

Problem (4), subject to the constraints in (3), was solved using the same hybrid approach as in the single-objective cases. In each iteration, the values of $V(X)$, $P(X)$, and $\theta_c$ were predicted utilizing the trained machine learning models.

Optimal solutions were found for various values of $\alpha$. Several Experimental results are summarized in Table I.

TABLE I. OPTIMIZATION RESULTS FOR PROBLEM (4)

| N | $\alpha$ | $f^*(X)$ | $V^*(X)$ | $P^*(X)$ | $X^*$ |
|---|---|---|---|---|---|
| 1 | 0.8 | 0.2414 | 236.7 | 1980.4 | (1.10000000, 1.75000000, 0.77579313, 1.10000000, 0.05000000, 1.58975295, 1.20000000) |
| 2 | 0.6 | 0.3231 | 255.88 | 1804.6 | (1.10000000, 1.75000000, 0.80000000, 1.10000000, 0.05000000, 1.72968288 1.20000000) |
| 3 | 0.5 | 0.3719 | 378.0 | 1400.0 | (1.10000000, 1.77500000, 0.80000000, 1.10000000, 0.05000000, 1.67826543 1.10000000) |
| 4 | 0.4 | 0.3245 | 438.47 | 1193.2 | (1.10000000, 1.80000000, 0.80000000, 1.10000000, 0.05000000, 1.61667915, 1.07503052) |
| 5 | 0.2 | 0.1865 | 489.11 | 1082.9 | (1.07523754, 1.79024608, 0.79999263, 1.10000000, 0.04347534, 1.63473464, 1.05622817) |

The structural dimensions of the electromagnet in Figure 1 are also presented for the solutions of single-objective problems (1) and (2), and the bi-objective problem (4) with $\alpha = 0.5$. The results outlined in Table II reveal several important trends and trade-offs inherent to electromagnet design optimization. Although the solution to Problem (1) yields the lowest material cost ($177.51), it comes at the expense of a significantly higher power consumption (2165.2 W). In contrast, the optimal design for Problem (2) drastically reduces the power usage to 1018.56 W, but increases the total material cost to $520. The bi-objective optimization (Problem 4) offers a balanced compromise, particularly when $\alpha = 0.5$, where the resulting cost and power values were $378 and 1400 W, falling within acceptable engineering thresholds. This solution is particularly valuable for real-world applications, where budget and energy efficiency must be jointly optimized.

Furthermore, the slight variations in structural coefficients among the three optimal designs underscore performance sensitivity to geometric proportions. For instance, the winding dimensions ($h_w$ and $l_w$) increase in the power-minimizing design, implying a trade-off between thermal management and material usage. Such insights can guide engineers in selecting design parameters that are best suited to the specific operational constraints of the application.

TABLE II. STRUCTURAL DIMENSIONS, COST, AND POWER VALUES OBTAINED FROM THE SOLUTIONS OF PROBLEMS (1), (2), (4)

| **Parameter** | **Problem (1)** | **Problem (2)** | **Problem (4)** |
|---|---|---|---|
| $a_c$ (m) | 0.1163166 | 0.13019378 | 0.1189738 |
| $b_c$ (m) | 0.1277505 | 0.14273211 | 0.1308712 |
| $l_c$ (m) | 0.1914338 | 0.2343488 | 0.2111785 |
| $b_a$ (m) | 0.0927724 | 0.10765779 | 0.1046970 |
| $b_{bc}$ (m) | 0.1403978 | 0.15700532 | 0.1439583 |
| $\Delta_w$ (m) | 0.0095143 | 0.01171744 | 0.0105589 |
| $h_w$ (m) | 0.0395218 | 0.06362604 | 0.0546613 |
| $l_w$ (m) | 0.0640924 | 0.10016243 | 0.0917361 |
| $l_{bc}$ (m) | 0.3235934 | 0.38962664 | 0.3574786 |
| $P$ (Wt) | 2165.20 | 1018.56 | 1400 |
| $V$ ($) | 177.510 | 520.000 | 378.0 |

## IV. CONCLUSION

This study introduced a hybrid machine learning–heuristic optimization framework for electromagnet design, aimed at reducing both material cost and operational energy consumption. The results confirm that combining heuristic search algorithms with neural network models improves both the computational speed and solution quality compared to standalone heuristic methods. The neural network–based hybrid model enables rapid evaluation of design alternatives, accelerating optimization and reducing reliance on computationally intensive simulations. The proposed framework provides flexibility in balancing material usage and operational efficiency, making it suitable for diverse application-specific requirements.

Compared to related works, the main advantage of this study lies in adopting a hybrid strategy that combines heuristic optimization with machine learning models. While surrogate-based methods, such as Kriging-assisted models [2] or Gaussian Processes [3], achieve high predictive accuracy, their scalability is limited due to the need for frequent retraining or kernel reconfiguration when the design domain changes. In contrast, the proposed neural network–enhanced framework generalizes effectively across the design space, adapting to new parameter ranges without compromising predictive fidelity. This capability is particularly beneficial in industrial contexts requiring rapid iteration and multi-scenario exploration.

Furthermore, unlike many single-objective formulations in electromagnetic design, for instance, on minimizing power loss [4] or superconductor volume [11], the proposed method integrates both single- and bi-objective optimization within a unified framework. This expands the scope of feasible design alternatives and enhances robustness by explicitly mapping the Pareto front between competing objectives. Compared to evolutionary multi-objective methods [12] or analytical FEM hybrids [10], the proposed approach reduces dependency on domain-specific modeling while maintaining computational efficiency. In this way, the methodology bridges high-fidelity physics-based optimization [8, 13] with data-driven design, offering a versatile tool for both conventional and advanced electromagnet systems.

Future work will focus on extending the framework to dynamic operating conditions and incorporating uncertainty-aware optimization.

## ACKNOWLEDGMENT

This work was supported by the Higher Education and Science Committee of the Republic of Armenia under research project No. 25RG-2B089.

## REFERENCES

[1] Q. N. Duc *et al.*, "Electromagnetic Parameters of IPM Motors based on the Genetic Algorithm Technique," *Engineering, Technology & Applied Science Research*, vol. 15, no. 3, pp. 23855–23861, June 2025, https://doi.org/10.48084/etasr.10559.

[2] W. Zhao, H. Shen, W. Chai, X. Wang, and B. Kwon, "Optimal Design and Experimental Test of a SPM Motor with Cost-Effective Magnet Utilization to Suppress Torque Pulsations," *IEEE Transactions on Magnetics*, vol. 54, no. 11, pp. 1–5, Nov. 2018, https://doi.org/10.1109/TMAG.2018.2842714.

[3] G. Choi, G.-H. Jang, M. Choi, J. Kang, Y. G. Kang, and S. Kim, "Optimal Design of a Surface Permanent Magnet Machine for Electric Power Steering Systems in Electric Vehicle Applications using a Gaussian Process-Based Approach," *Actuators*, vol. 13, no. 1, Dec. 2023, Art. no. 13, https://doi.org/10.3390/act13010013.

[4] Y. Song *et al.*, "Optimization Design of DC Electromagnet Coil Considering the Power Consumption and Cost," *IEEJ Transactions on Electrical and Electronic Engineering*, vol. 19, no. 8, pp. 1420–1428, Aug. 2024, https://doi.org/10.1002/tee.24089.

[5] Y. Li, G. Lei, G. Bramerdorfer, S. Peng, X. Sun, and J. Zhu, "Machine Learning for Design Optimization of Electromagnetic Devices: Recent Developments and Future Directions," *Applied Sciences*, vol. 11, no. 4, Feb. 2021, Art. no. 1627, https://doi.org/10.3390/app11041627.

[6] W. Liu *et al.*, "Structural Optimization and Electromagnetic Performance Research of Axial Magnetic Field Tidal Current Generators," *Energies*, vol. 18, no. 10, May 2025, Art. no. 2520, https://doi.org/10.3390/en18102520.

[7] Z. Hao, Y. Ma, P. Wang, G. Luo, and Y. Chen, "A Review of Axial-Flux Permanent-Magnet Motors: Topological Structures, Design, Optimization and Control Techniques," *Machines*, vol. 10, no. 12, Dec. 2022, Art. no. 1178, https://doi.org/10.3390/machines10121178.

[8] Z. Yang *et al.*, "Optimized Design and Electromagnetic-Thermal-Mechanical Analysis of a Toroidal D-Shaped Superconducting Magnet in 5 MW LIQHY-SMES System," *IEEE Transactions on Applied Superconductivity*, vol. 34, no. 3, pp. 1–7, May 2024, https://doi.org/10.1109/TASC.2024.3376491.

[9] D. Q. Nguyen, L. D. Hai, D. B. Minh, and V. D. Quoc, "Analysis of Electromagnetic Parameters of Hybrid Externally Excited Synchronous Motors for Electric Vehicle Applications," *Engineering, Technology & Applied Science Research*, vol. 13, no. 3, pp. 10670–10674, June 2023, https://doi.org/10.48084/etasr.5824.

[10] P. R. Raut, H. J. Bahirat, and M. D. Atrey, "Analytical Approach for Optimal HTS Solenoid Design," *IEEE Transactions on Applied Superconductivity*, vol. 31, no. 2, pp. 1–9, Mar. 2021, https://doi.org/10.1109/TASC.2020.3038531.

[11] Z. Liang, "An Optimal Design of Actively Shielded MRI Superconducting Magnet," *IEEE Transactions on Applied Superconductivity*, vol. 29, no. 2, pp. 1–4, Mar. 2019, https://doi.org/10.1109/TASC.2018.2883676.

[12] A. H. K. Asadi, A. Jahangiri, M. Zand, M. Eskandari, M. A. Nasab, and H. Meyar-Naimi, "Optimal Design of High Density HTS-SMES Step-Shaped Cross-Sectional Solenoid to Mechanical Stress Reduction," in *2022 International Conference on Protection and Automation of Power Systems*, Zahedan, Iran, Islamic Republic of, Jan. 2022, pp. 1–6, https://doi.org/10.1109/IPAPS55380.2022.9763198.

[13] S. P. Filippidis, A. S. Bouhouras, N. Poulakis, T. Theodoulidis, and G. C. Christoforidis, "Overview of the Electromagnetic Optimization Literature of Superconducting Solenoidal Magnets and Coils," *IEEE Transactions on Applied Superconductivity*, vol. 33, no. 7, pp. 1–21, Oct. 2023, https://doi.org/10.1109/TASC.2023.3280822.

[14] H. Tiismus, A. Kallaste, T. Vaimann, and A. Rassõlkin, "State of the Art of Additively Manufactured Electromagnetic Materials for Topology Optimized Electrical Machines," *Additive Manufacturing*, vol. 55, July 2022, Art. no. 102778, https://doi.org/10.1016/j.addma.2022.102778.

[15] F. Lucchini, R. Torchio, V. Cirimele, P. Alotto, and P. Bettini, "Topology Optimization for Electromagnetics: A Survey," *IEEE Access*, vol. 10, pp. 98593–98611, 2022, https://doi.org/10.1109/ACCESS.2022.3206368.

[16] A. Hashemi and P. Yazdanpanah Qaraei, "Multi-Coil Electromagnets: An Accurate Magnetic Equivalent Circuit, Cost, and Energy Management," *International Journal of Numerical Modelling: Electronic Networks, Devices and Fields*, vol. 34, no. 4, July 2021, Art. no. e2868, https://doi.org/10.1002/jnm.2868.

[17] D. Matajira-Rueda, J. M. Cruz-Duarte, J. G. Avina-Cervantes, M. A. Ibarra-Manzano, and R. Correa, "Optimization-Based Strategies for Optimal Inverse Parameters Estimation for Heat Transfer Systems," *IEEE Access*, vol. 9, pp. 71328–71343, 2021, https://doi.org/10.1109/ACCESS.2021.3079367.

[18] I. Patel *et al.*, "Stochastic Optimisation and Economic Analysis of Combined High Temperature Superconducting Magnet and Hydrogen Energy Storage System for Smart Grid Applications," *Applied Energy*, vol. 341, July 2023, Art. no. 121070, https://doi.org/10.1016/j.apenergy.2023.121070.

[19] A. K. Grigoryan, A. G. Avetisyan, N. H. Chukhajyan, A. A. Hovhannisyan, and A. A. Hovsepyan, "Optimal Design of an Electromagnet using Machine Learning Methods," *International Review of Electrical Engineering*, vol. 19, no. 4, Aug. 2024, Art. no. 337, https://doi.org/10.15866/iree.v19i4.25425.

[20] A. K. Grigoryan, A. G. Avetisyan, T. R. Melkonyan, A. A. Hovhannisyan, and A. A. Hovsepyan, "Optimization of Parameters of Electromagnetic System with Magnetorheological Fluid," *International Review of Electrical Engineering*, vol. 19, no. 5, Oct. 2024, Art. no. 410, https://doi.org/10.15866/iree.v19i5.25645.

[21] A. Grigoryan, A. Avetisyan, T. Melkonyan, and K. Yenokyan, "Automated Modeling of an Electromagnet with Magnetorheological Fluid," *Engineering, Technology & Applied Science Research*, vol. 15, no. 3, pp. 22937–22944, Jun. 2025, https://doi.org/10.48084/etasr.10909.

[22] X.-S. Yang, "Multi-Objective Optimization," in *Nature-Inspired Optimization Algorithms*, Amsterdam, Netherlands: Elsevier, 2014, pp. 197–211, https://doi.org/10.1016/B978-0-12-416743-8.00014-2.